POTSDAM-INSTITUT FÜR KLIMAFOLGENFORSCHUNG

PIK

Originally published as:

Du, M., Wei, J., Li, M.-Y., Gao, Z.-k., Kurths, J. (2023): Interconnected ordinal pattern complex network for characterizing the spatial coupling behavior of gas-liquid two-phase flow. - Chaos, 33, 6, 063108.

DOI: https://doi.org/10.1063/5.0146259

Chaos
An Interdisciplinary Journal of Nonlinear Science

RESEARCH ARTICLE | JUNE 05 2023

Interconnected ordinal pattern complex network for characterizing the spatial coupling behavior of gas–liquid two-phase flow

Special Collection: Ordinal Methods: Concepts, Applications, New Developments and Challenges

Meng Du ; Jie Wei ; Meng-Yu Li ; Zhong-ke Gao ; Jürgen Kurths

Check for updates

Chaos 33, 063108 (2023)
https://doi.org/10.1063/5.0146259

View Online
Export Citation
CrossMark

08 December 2023 12:53:02

AIP Publishing

Chaos ARTICLE scitation.org/journal/cha

Interconnected ordinal pattern complex network for characterizing the spatial coupling behavior of gas–liquid two-phase flow

Cite as: Chaos 33, 063108 (2023); doi: 10.1063/5.0146259
Submitted: 12 February 2023 · Accepted: 11 May 2023 ·
Published Online: 5 June 2023

View Online Export Citation CrossMark

Meng Du,[1,a)] Jie Wei,[1,b)] Meng-Yu Li,[2,c)] Zhong-ke Gao,[2,d)] and Jürgen Kurths[3,4,e)]

AFFILIATIONS

[1]School of Electrical Engineering and Automation, Tianjin University of Science and Technology, Tianjin 300222, China
[2]School of Electrical Engineering and Automation, Tianjin University, Tianjin 300072, China
[3]Research Department Complexity Science, Potsdam Institute for Climate Impact Research, 14473 Potsdam, Germany
[4]Institute of Physics, Humboldt University of Berlin, 12489 Berlin, Germany

Note: This paper is part of the Focus Issue on Ordinal Methods: Concepts, Applications, New Developments and Challenges.
[a)]**Author to whom correspondence should be addressed:** mdu@tust.edu.cn
[b)]**Electronic mail:** zj674022840@outlook.com
[c)]**Electronic mail:** xyblmy@tju.edu.cn
[d)]**Electronic mail:** zhongkegao@tju.edu.cn
[e)]**Electronic mail:** Juergen.Kurths@pik-potsdam.de

08 December 2023 12:53:02

ABSTRACT

The complex phase interactions of the two-phase flow are a key factor in understanding the flow pattern evolutional mechanisms, yet these complex flow behaviors have not been well understood. In this paper, we employ a series of gas–liquid two-phase flow multivariate fluctuation signals as observations and propose a novel interconnected ordinal pattern network to investigate the spatial coupling behaviors of the gas–liquid two-phase flow patterns. In addition, we use two network indices, which are the global subnetwork mutual information (I) and the global subnetwork clustering coefficient (C), to quantitatively measure the spatial coupling strength of different gas–liquid flow patterns. The gas–liquid two-phase flow pattern evolutionary behaviors are further characterized by calculating the two proposed coupling indices under different flow conditions. The proposed interconnected ordinal pattern network provides a novel tool for a deeper understanding of the evolutional mechanisms of the multi-phase flow system, and it can also be used to investigate the coupling behaviors of other complex systems with multiple observations.

Published under an exclusive license by AIP Publishing. https://doi.org/10.1063/5.0146259

In many complex systems, coupling phenomena are frequently observed, when two or more parts in the system are interacting with each other. As for the complex multi-phase flow, the coupling behavior between the immiscible phases is influenced by many factors, making it difficult to get a clear description of the dynamics of the multi-phase flow system. In this paper, we design a flow loop experiment to investigate the coupling behaviors of the vertical gas–liquid two-phase flow system. We use a recently proposed popular tool, which is the interconnected ordinal pattern complex network to model the experimental data. We also employ two indices, the subnetwork mutual information and the subnetwork clustering coefficient, to qualify the spatial coupling strength of different gas–liquid two-phase flow patterns. This work clarifies the coupling behaviors of different gas–liquid two-phase flow patterns and provides an efficient tool for characterizing multi-phase flow systems.

I. INTRODUCTION

The mixed flowing of gas and water in pipes yields typical gas–liquid two-phase flows, which are widely present in the fields of petroleum,[1] biology,[2] hydraulics,[3] chemical,[4] energy,[5] and so on. Understanding the morphological characteristics of the two immiscible phases, which are known as flow patterns, is of great

Published under an exclusive license by AIP Publishing

importance for the design of the flowing control system. However, the gas–liquid two-phase flow is such a complex system that there are only a few precise analytic models suitable for interpreting the complex dynamics of diverse flow patterns. Hence, plenty of researchers have shifted to experimental methods to investigate the dynamics of gas–liquid two-phase flows in various channels, such as vertical pipes,[6] horizontal pipes,[7] inclined pipes,[8] porous media,[9] fluidized bed,[10] and micro-fluidic chip.[11] To reveal the hidden fluid dynamics from the experimental observations, many data analysis tools, including time–frequency spectrum,[12] recurrence plot,[13] complex network,[14] nonlinear analysis,[15] multi-scale analysis,[16] and wavelet analysis,[17] have been applied, and various two-phase flow characteristics, such as flow pattern complexity,[18] flow pattern irreversibility,[19] flow pattern transition dynamics,[20] fluid multi-scale dynamics,[21] fluid stability,[22] and the flow pattern determinism[23] have been clarified. One inherent characteristic of a two-phase flow pattern is the spatial coupling behaviors of the two immiscible phases, which is a key factor for indicating the evolutionary dynamics of the gas–liquid two-phase flow patterns. However, few studies on the detection of coupling dynamics from two-phase flow experimental data have been reported, and the flow pattern spatial coupling behaviors still require more detailed clarification. Note that analyzing the correlations of the experimental multivariate observations is an effective way to characterize the coupling behaviors of a complex system. To date, various tools, including transfer entropy,[24] mutual information,[25] phase dynamics modeling,[26] state space topography,[27] and polynomial transfer functions,[28] have been employed to analyze the experimental multivariate data, which are then used to identify the coupling dynamics of diverse complex systems.[29–31]

Recently, the complex network is shown as a powerful tool for modeling the experimental data observed from various complex systems.[32–34] As for the multi-phase flow system, the networks reconstructed from fluid fluctuation signals have also been successfully applied to identify the dynamics of the mixed fluid.[15,35] In particular, recent research studies broadened the topology of the complex network to the multilayered configuration,[36] which is assumed more efficient not only to detect the dynamics of the whole system but also to characterize the interaction behaviors between the subsystems. Now, the interconnected multilayer complex network configuration has been successfully applied to model the experimental data observed from various interacted complex systems, such as the software,[37] public transport,[38] hemodynamic,[39] community,[40] and climate changes.[41] It is worth noting that the complex multiphase flow dynamic behaviors are effectively characterized by the experimentally measured multivariate signals,[42] and it seems that properly modeling the correlations among each measured univariate signal provides a solution for revealing the coupling behaviors of the multi-phase flow system.

In this paper, we first conduct a vertical gas–liquid two-phase flow experiment to collect the multivariate fluid fluctuation signals. Then, we propose an interconnected ordinal pattern complex network to characterize the inherent coupling behaviors of the gas–liquid two-phase flow patterns. It can be considered as a collection of interacted ordinal pattern transitional networks, which are established with the experimentally collected multivariate fluid fluctuation signals. The fundamental configuration of each individual ordinal pattern network, which was first proposed by Michael Small,[43] has recently been applied in many fields, such as fluid,[44] ECG data,[45] climate,[46] turbulent coaxial jet,[47] and flame.[48,49] As a light weighted and fast computing network, the ordinal pattern network is a powerful tool for modeling noisy experimental observations, e.g., the contaminated two-phase flow fluctuation signals. We also employ two interconnected ordinal pattern network coupling indices, which are the global subnetwork mutual information (I) and the global subnetwork clustering coefficient (C), to quantify the spatial coupling strength among different flow patterns, and the flow pattern evolutional dynamics are also interpreted with the calculated indices, under different flow conditions.

The remainder of this paper is organized as follows. In Sec. II, we introduce our gas–liquid two-phase flow experiment and the collected multivariate fluid fluctuation signals. In Sec. III, we give a description of the construction method of the gas–liquid two-phase flow interconnected ordinal pattern network. In Sec. IV, the spatial coupling behaviors the gas–liquid two-phase flow patterns are analyzed. The conclusions are in Sec. V.

II. THE GAS–LIQUID TWO-PHASE FLOW EXPERIMENT

As shown in Fig. 1, we design and carry out a flow loop experiment in a vertical 50 mm inner diameter pipe to collect the multivariate conductance fluctuation signals of the gas–liquid two-phase flow, which are further employed to investigate the spatial coupling behaviors of different flow patterns. In the experiment, water and gas are simultaneously induced into a 50 mm inner-diameter vertical testing pipe to generate the desired flow patterns. The water flow rate is adjusted with a metering pump, while the gas flow rate is controlled with an actuated valve and metered with a gas flowmeter.

We employ a four-sector conductance sensor,[50] which is embedded in the vertical testing pipe, to measure the multivariate fluctuations of the gas–liquid two-phase flow. As shown in Fig. 1, the four-sector conductance sensor consists of four pairs of electrodes (E_A and M_A, E_B and M_B, and E_C and M_C, and E_D and M_D). The stimulating electrodes E_A, E_B, E_C, and E_D are connected to a 100 KHz sinusoidal signal generator, and M_A, M_B, M_C, and M_D are the measuring electrodes. Each pair electrode is an individual conductance sensor, which is designed sensitively to the fluid fluctuations in a quadrant area of the pipe cross section. We use these electrode sensors to measure the gas–liquid two-phase flow fluctuations and obtain a series of four-channel conductance fluctuation time series. In the experiment, we use four independent measurement systems to collect the conductance fluctuation signals on the electrode pairs of the four-sector conductance sensor. We repeatedly carry out this experiment under various flow conditions, of which the water flow rate is in the range of 0.22–23 l/min, and the gas flow rate is in the range of 0.3472–0.4862 l/min.

As shown in Fig. 2, we observe three typical gas–liquid two-phase flow patterns in this two-phase flow experiment, which are the slug flow, the non-uniform bubble flow, and the uniform bubble flow. (i) **Slug flow:** observed at a lower mixture flow rate, Taylor bubbles with a diameter almost equal to the pipe diameter are periodically observed in the testing pipe, and each Taylor bubble

08 December 2023 12:53:02

Published under an exclusive license by AIP Publishing

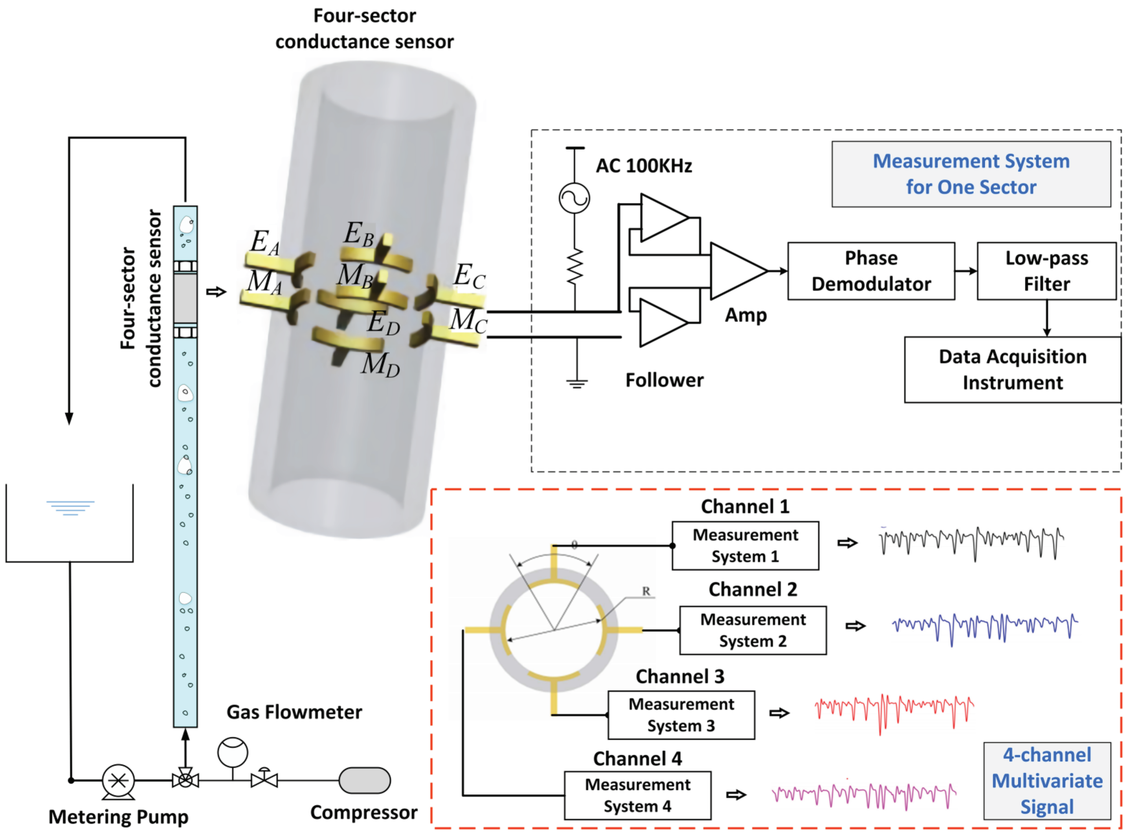

FIG. 1. The schematic of the gas–liquid two-phase flow loop experiment.

08 December 2023 12:53:02

is followed by a cluster of small gas bubbles. (ii) **Non-uniform bubble flow:** also known as the slug-bubble transition flow, spherically capped bubbles intermittently pass through the testing pipe. (iii) **Uniform bubble flow:** observed at a higher mixture rate, small gas bubbles are uniformly distributed, and the mixed fluid show homogeneous characteristics.

As shown in Fig. 3(a), the multivariate conductance signals of the slug flow fluctuate periodically, indicating the motion of the intermittent gas slugs. Meanwhile, we observe obvious synchronized fluctuation characteristics of the univariate signals. It indicates that there exist some sort of local similarities in the structure of slug flow. Figure 3(b) shows the measured multivariate conductance fluctuation signals of the non-uniform bubble flow. As we can see, similar to that of slug flow, the fluctuations of the non-uniform bubble flow also exhibit periodic characteristics, indicating the intermittently observed spherically capped bubbles. We also find synchronized fluctuation behaviors from the multivariate signals of non-uniform bubble flow, i.e., there still exist some local similarities of the non-uniform bubble flow. As shown in Fig. 3(c), the experimentally collected multivariate conductance signals of the uniform bubble flow are noisy like, reflecting the stochastic flowing behaviors

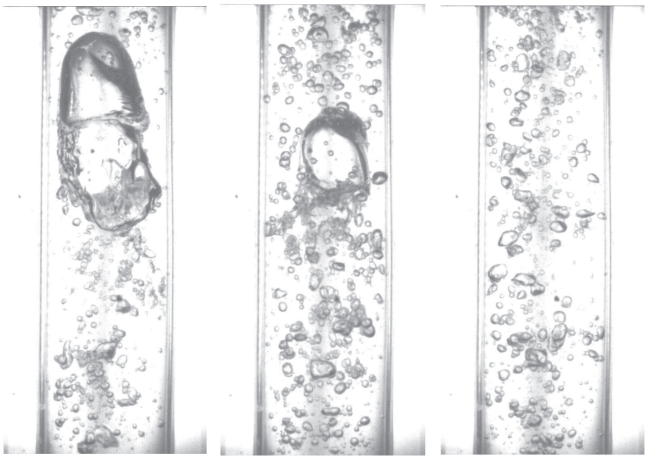

(a) (b) (c)

FIG. 2. The snapshot of the different gas–liquid two-phase flow patterns. (a) Slug flow. (b) Non-uniform bubble flow. (c) Uniform bubble flow.

Published under an exclusive license by AIP Publishing

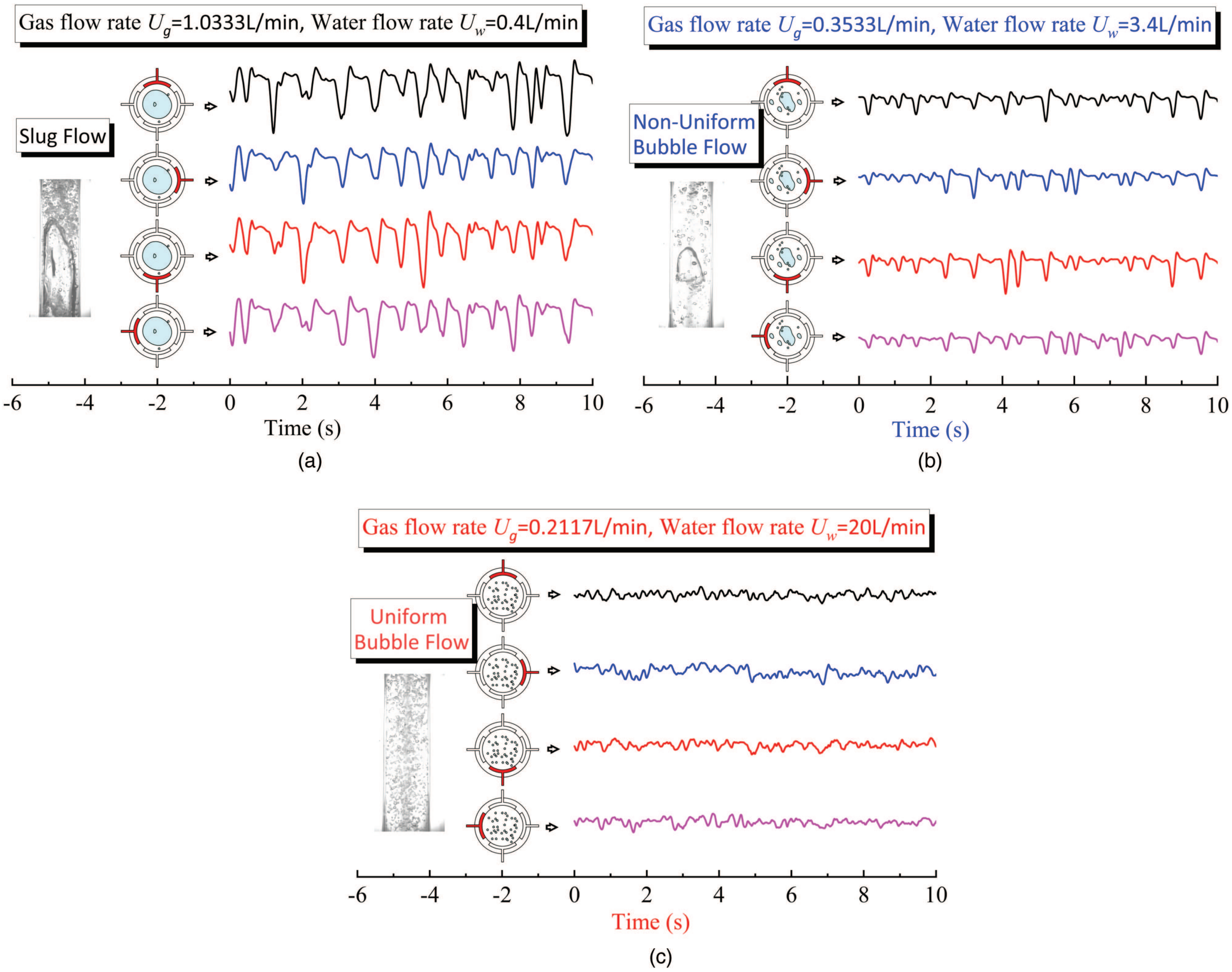

FIG. 3. The multivariate conductance fluctuation signals of the gas–liquid two-phase flows. (a) Slug flow. (b) Non-uniform bubble flow. (c) Uniform bubble flow. (a) scale=0.5, (b) scale=0.5, (c) scale=0.5.

of this homogeneous flow pattern. Furthermore, we find that each measured univariate signal of uniform bubble flow is uncorrelated, indicating that the small and uniformly distributed gas bubbles are flowing in an unsynchronized way.

III. THE GAS–LIQUID TWO-PHASE FLOW INTERCONNECTED ORDINAL PATTERN NETWORKS

We construct a series of interconnected ordinal pattern complex networks from the collected four-channel multivariate fluctuation signals to characterize the dynamic flow behaviors of different gas–liquid two-phase flow patterns. Figure 4 shows the schematic diagram for establishing an interconnected ordinal pattern network from the multivariate fluctuation signal.

Given the experimentally measured gas–liquid two-phase flow four-channel multivariate signal $s^{\alpha}(n)$ of length l,

$$s^{\alpha}(n); \alpha \in [1, 2, 3, 4]; n \in [1, l]. \tag{1}$$

We first reconstruct the multivariate phase-space vector with the standard delay coordinate embedding method,[51]

$$\overrightarrow{S^{\alpha}}(t) = [s^{\alpha}(t), s^{\alpha}(t+\tau), \ldots, s^{\alpha}(t+(D-1)\cdot\tau)],$$
$$t \in [1, l-(D-1)\cdot\tau], \tag{2}$$

where D is the reconstructed dimension and τ refers to the delay time. We then associate each reconstructed vector with a symbol, which is the permutation order of the elements in $\vec{S}^{\alpha}(t)$. These permutations are also known as ordinal patterns,[52] and there exists a

Published under an exclusive license by AIP Publishing
08 December 2023 12:53:02

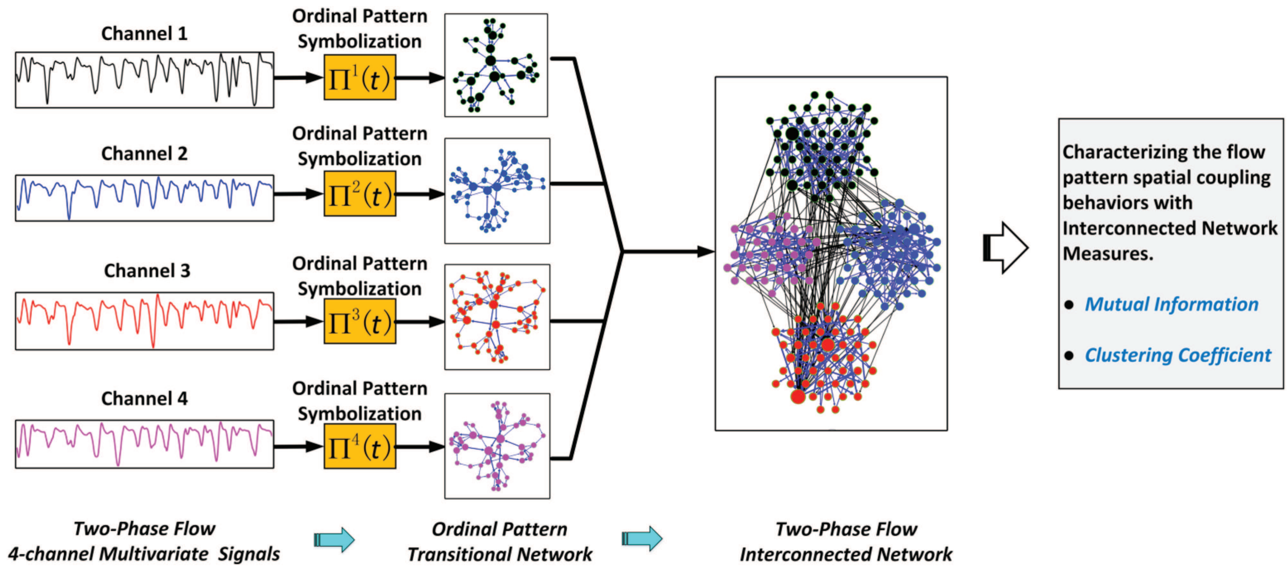

FIG. 4. The schematic diagram of gas–liquid two-phase flow interconnected ordinal pattern network.

total of $D!$ kinds of possible ordinal patterns in the reconstructed phase space. The ordinal pattern set is expressed as

$$X^{\alpha} = \left\{x_1^{\alpha}, x_2^{\alpha}, \ldots, x_p^{\alpha}\right\}, \tag{3}$$

where $p = D!$, and the elements in X^{α} are all the possible ordinal patterns derived from $\vec{S}^{\alpha}(t)$.With this ordinal symbolization, the multivariate phase-space vector series $\vec{S}^{\alpha}(t)$ is transformed into a multivariate symbolic sequence $\Pi^{\alpha}(t)$, which is expressed as

$$\prod^{\alpha}(t) = [\pi_1^{\alpha}, \pi_2^{\alpha}, \ldots, \pi_{l-(D-1)\cdot\tau}^{\alpha}], \tag{4}$$

where each symbol π_t^{α} in $\Pi^{\alpha}(t)$ comes from the permutation orders of its corresponding phase-space vector $\vec{S}^{\alpha}(t)$.

Our proposed gas–liquid two-phase flow interconnected ordinal pattern network can be expressed as a pair,

$$G = \{V, E\}, \tag{5}$$

where $V = \{v^{\alpha};\ \alpha \in [1, 2, 3, 4]\}$ is a family of correlated subnetworks, and each subnetwork v^{α} is a typical single layered ordinal pattern transition network,[43] which is established by the αth univariate symbolic series of $\Pi^{\alpha}(t)$. E refers to the interconnections that link the nodes between each subnetwork v^{α}. The nodes of each subnetwork v^{α} come from the ordinal pattern set X^{α}, which contains a total of $D!$ kinds of ordinal patterns. When reconstructing the multivariate phase-space vector, we choose a fixed embedded dimension for each univariate signal, so that the established subnetworks share the same node set, which is expressed as

$$X = X^1 = X^2 = X^3 = X^4, \tag{6}$$

The adjacent matrix of each subnetwork v^{α} is expressed as

$$(d_{ij}^{\alpha}) = \begin{bmatrix} d_{11}^{\alpha} & d_{12}^{\alpha} & \cdots & d_{1p}^{\alpha} \\ d_{21}^{\alpha} & d_{22}^{\alpha} & \cdots & d_{2p}^{\alpha} \\ \vdots & \vdots & \ddots & \vdots \\ d_{p1}^{\alpha} & d_{p2}^{\alpha} & \cdots & d_{pp}^{\alpha} \end{bmatrix}, \tag{7}$$

where d_{ij}^{α} denotes the weighted edge from the ith node to the jth node in the subnetwork v^{α}, which is determined by the following equation:

$$d_{ij}^{\alpha} = \frac{N_{ij}^{\alpha}}{T-1}, \tag{8}$$

where N_{ij}^{α} is the number of enumerated sequential adjacent ordinal pattern pairs $\left[x_i^{\alpha},\ x_j^{\alpha}\right]$, which exist in the symbolic series $\Pi^{\alpha}(t)$, and T is the length of $\Pi^{\alpha}(t)$.

The interactions among the subnetworks of G are modeled with the matrix set,

$$E = \left\{(e_{ij}^{\alpha\beta}), \alpha < \beta, \alpha, \beta \in [1, 2, 3, 4]\right\}, \tag{9}$$

$(e_{ij}^{\alpha\beta})$ is the interlayer adjacent matrix, which denotes the weighted connections between subnetwork v^{α} and v^{β},

$$(e_{ij}^{\alpha\beta}) = \begin{bmatrix} e_{11}^{\alpha\beta} & e_{12}^{\alpha\beta} & \cdots & e_{1p}^{\alpha\beta} \\ e_{21}^{\alpha\beta} & e_{22}^{\alpha\beta} & \cdots & e_{2p}^{\alpha\beta} \\ \vdots & \vdots & \ddots & \vdots \\ e_{p1}^{\alpha\beta} & e_{p2}^{\alpha\beta} & \cdots & e_{pp}^{\alpha\beta} \end{bmatrix}, \tag{10}$$

where $e_{ij}^{\alpha\beta}$ denotes the edge, which connects the node x_i^{α} in subnetwork v^{α} and node x_j^{β} in subnetwork v^{β}, and the interconnected

08 December 2023 12:53:02

Published under an exclusive license by AIP Publishing

weight can be defined as

$$e_{ij}^{\alpha\beta} = P(x_i^\alpha \,|\, x_j^\beta) = \frac{M_{ij}^{\alpha\beta}}{T}, \tag{11}$$

where $M_{ij}^{\alpha\beta}$ is the number of enumerated contemporaneously observed pair $\left[x_i^\alpha,\ x_j^\beta\right]$ in both the symbolic series $\Pi^\alpha(t)$ and $\Pi^\beta(t)$, and T denotes the length of the multivariate ordinal pattern time series.

In this work, we choose the embedded dimension $D = 6$ based on distinguishing false nearest neighbors (FNNs),[53] and we use the correlation-integral-based method[54] to determine the delay time $\tau = 1$, i.e., one sampling duration. The sampling frequency of the fluid fluctuation time series is set to 2000 Hz, and we choose a duration of 30 s for the analysis, i.e., the time series used to construct the network has a length of $l = 60\,000$ points. According to the theory of Bandt and Pompe,[52] there will be a total of $D! = 720$ kinds of possible different ordinal patterns in each two-phase flow fluctuation signal, and the length of the ordinal sequence $\pi(t)$ is $l - (D-1)\cdot\tau = 59\,995$. The established gas–liquid two-phase flow interconnected complex networks are constituted of four subnetworks, and each of these subnetworks is a typical single layered ordinal pattern network with at most $D! = 720$ nodes. Although we choose a sufficiently long time series to establish the ordinal pattern interconnected network, some of the network nodes are still missing due to the existing flow pattern determinism characteristics.[23] We investigate the two-phase flow local evolutional dynamics by analyzing the topology characteristics of each subnetwork. We also characterize the flow pattern spatial coupling behaviors with the network interconnections, which link the interacted subnetworks.

IV. ANALYZING THE COUPLING BEHAVIORS OF GAS–LIQUID TWO-PHASE FLOW PATTERNS

Next, we employ two interconnected network indices, which are the subnetwork mutual information (I) and the subnetwork clustering coefficient (C), to quantitatively investigate the spatial coupling behaviors of the gas–liquid two-phase flow patterns. Given an interconnected ordinal pattern complex network $G = \{V, E\}$, we define *the subnetwork mutual information entropy* of the subnetwork v^α and v^β as

$$I^{\alpha\beta} = \sum_{i=1}^{p}\sum_{j=1}^{p} e_{ij}^{\alpha\beta}\cdot \log\frac{e_{ij}^{\alpha\beta}}{P(x_i^\alpha)\cdot P(x_j^\beta)}, \tag{12}$$

where $p = D!$ is the cardinality of the ordinal pattern set. $P(x_i^\alpha)$ and $P(x_j^\beta)$ denote the appearing probability of ordinal pattern x_i^α in the series $\Pi^\alpha(t)$ and the appearing probability of x_j^β in the series $\Pi^\beta(t)$, respectively. Then, we define the global subnetwork mutual information of interconnected network as the average of $I^{\alpha\beta}$ over all the subnetworks, which is expressed as

$$I = \frac{2}{k\cdot(k-1)} \sum_{\substack{\alpha\neq\beta \\ \alpha,\beta\in[1,k]}} I^{\alpha\beta}, \tag{13}$$

where $k = 4$ is the number of subnetworks in the established gas–liquid two-phase flow interconnected ordinal pattern network. The defined mutual information I measures the information shared between the subnetworks of the overall system. It also quantifies the coupling strength of the interacted subnetworks. A stronger coupling strength between the subnetworks implies larger I, while a lower value of I indicating weaker coupling behavior existed in the overall system.

The subnetwork clustering coefficient of the interconnected ordinal pattern network G is defined as the averaged inter-subnetwork clustering coefficient of all the network nodes. It quantifies the inter-subnetwork correlations of the nodes in each subnetwork. We first define the inter-subnetwork clustering coefficient of node x_i, which corresponds to the subnetwork v^α and v^β as

$$C_i^{\alpha\beta} = \frac{\sum_{\substack{j,r\in[1,p]\\ j\neq r}} e_{ij}^{\alpha\beta}\cdot e_{ir}^{\alpha\beta}\cdot d_{jr}^{\beta}}{\sum_{\substack{j,r\in[1,p]\\ j\neq r}} e_{ij}^{\alpha\beta}\cdot e_{ir}^{\alpha\beta}} + \frac{\sum_{\substack{j,r\in[1,p]\\ j\neq r}} e_{ji}^{\alpha\beta}\cdot e_{ri}^{\alpha\beta}\cdot d_{jr}^{\alpha}}{\sum_{\substack{j,r\in[1,p]\\ j\neq r}} e_{ji}^{\alpha\beta}\cdot e_{ri}^{\alpha\beta}}. \tag{14}$$

Then, we define the inter-subnetwork clustering coefficient of two coupled subnetworks as

$$C^{\alpha\beta} = \sum_{i=1}^{p} C_i^{\alpha\beta}. \tag{15}$$

The global subnetwork clustering coefficient C of the overall network G are defined as

$$C = \frac{2}{k\cdot(k-1)} \sum_{\substack{\alpha\in[1,k]\\ \beta\in[1,k]\\ \alpha<\beta}} C^{\alpha\beta}. \tag{16}$$

For the established interconnected ordinal pattern networks of the gas–liquid two-phase flow system, we calculate the inter-subnetwork mutual information $I^{\alpha\beta}$ and the inter-subnetwork clustering coefficient $C^{\alpha\beta}$ for every pair of subnetworks, which are shown in Fig. 5. Since the larger gas slugs existed in the slug flows retain an obvious stable spatial structure, the gas slug flows exhibit strongly coupling flow behaviors, resulting in a higher value of $I^{\alpha\beta}$ and $C^{\alpha\beta}$. When gas slugs evolve into non-uniform bubbles (spherically capped bubbles), the gas phase spatial stability is reduced, but not lost. In this regard, the non-uniform bubble flow still retains the coupled flowing behaviors but shows a slight decrease of $I^{\alpha\beta}$ and $C^{\alpha\beta}$. In the case of uniform bubble flow, the smaller gas bubbles are distributed uniformly and stochastically in the testing pipe, resulting in a weakly coupled flow behavior of the uniform bubble flow. Hence, its $I^{\alpha\beta}$ and $C^{\alpha\beta}$ are significantly reduced from those of the gas slug flow and the non-uniform bubble flow.

Figure 6 shows the estimated global subnetwork mutual information I and the global subnetwork clustering coefficient C of the gas–liquid two-phase flow interconnect complex networks. The gas–liquid two-phase flow pattern evolutionary dynamics are identified with these two coupling indices under different flow conditions. When gradually increasing the water flow rate, the flow pattern evolves from the slug flow via the non-uniform bubble flow, to the uniform bubble flow. As shown in Fig. 6, both I and C gradually decrease, which implies that the spatial coupling strength of the gas–liquid two-phase flow is not only related to the flow pattern but also the fluid turbulence intensity. Under lower water velocity,

08 December 2023 12:53:02

Published under an exclusive license by AIP Publishing

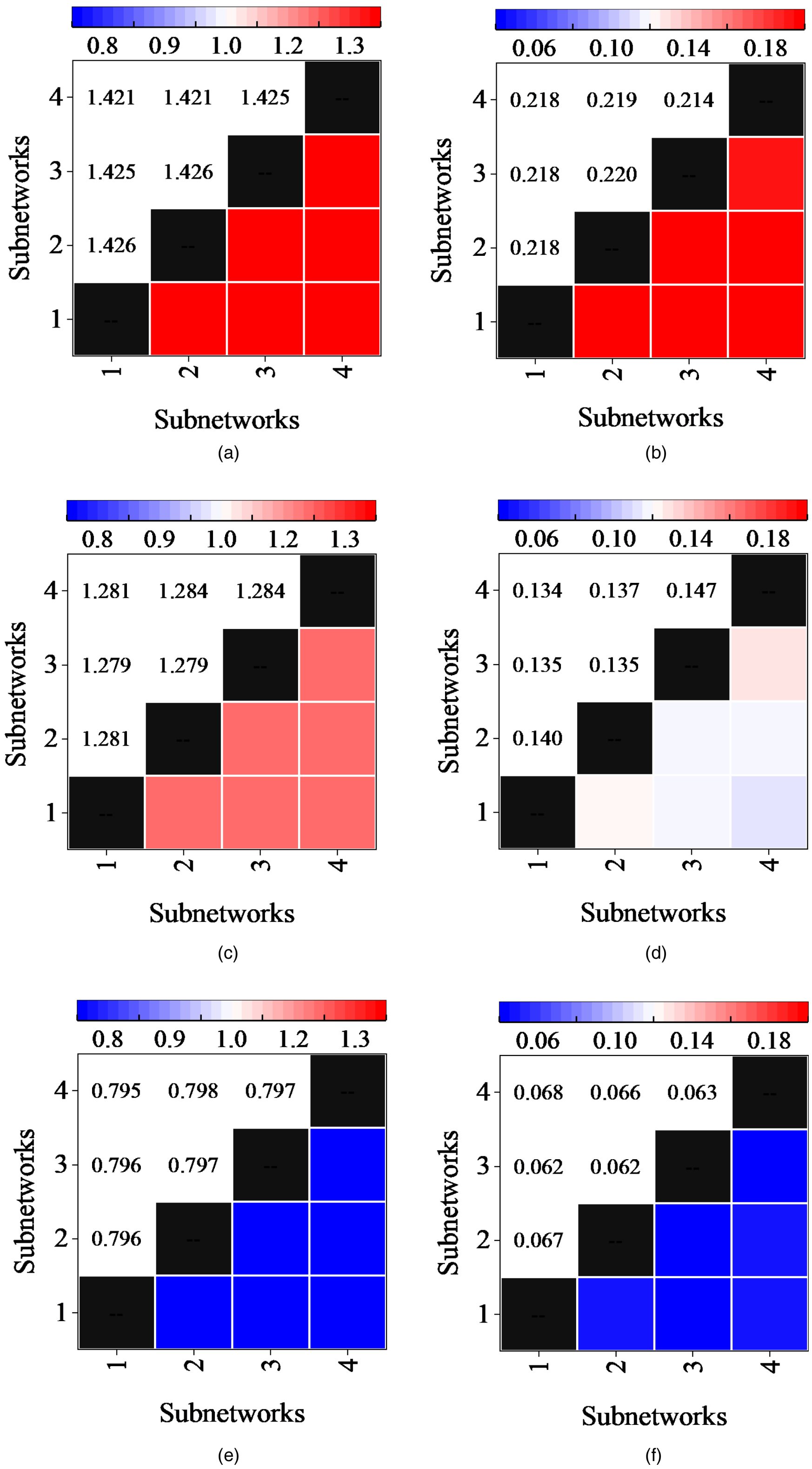

FIG. 5. The estimated coupling indices under different flow patterns. (a) The inter-subnetwork mutual information of the slug flow. (b) The inter-subnetwork clustering coefficient of the slug flow. (c) The inter-subnetwork mutual information of the non-uniform bubble flow. (d) The inter-subnetwork clustering coefficient of the non-uniform bubble flow. (e) The inter-subnetwork mutual information of the uniform bubble flow. (f) The inter-subnetwork clustering coefficient of the uniform bubble flow.

08 December 2023 12:53:02

Published under an exclusive license by AIP Publishing

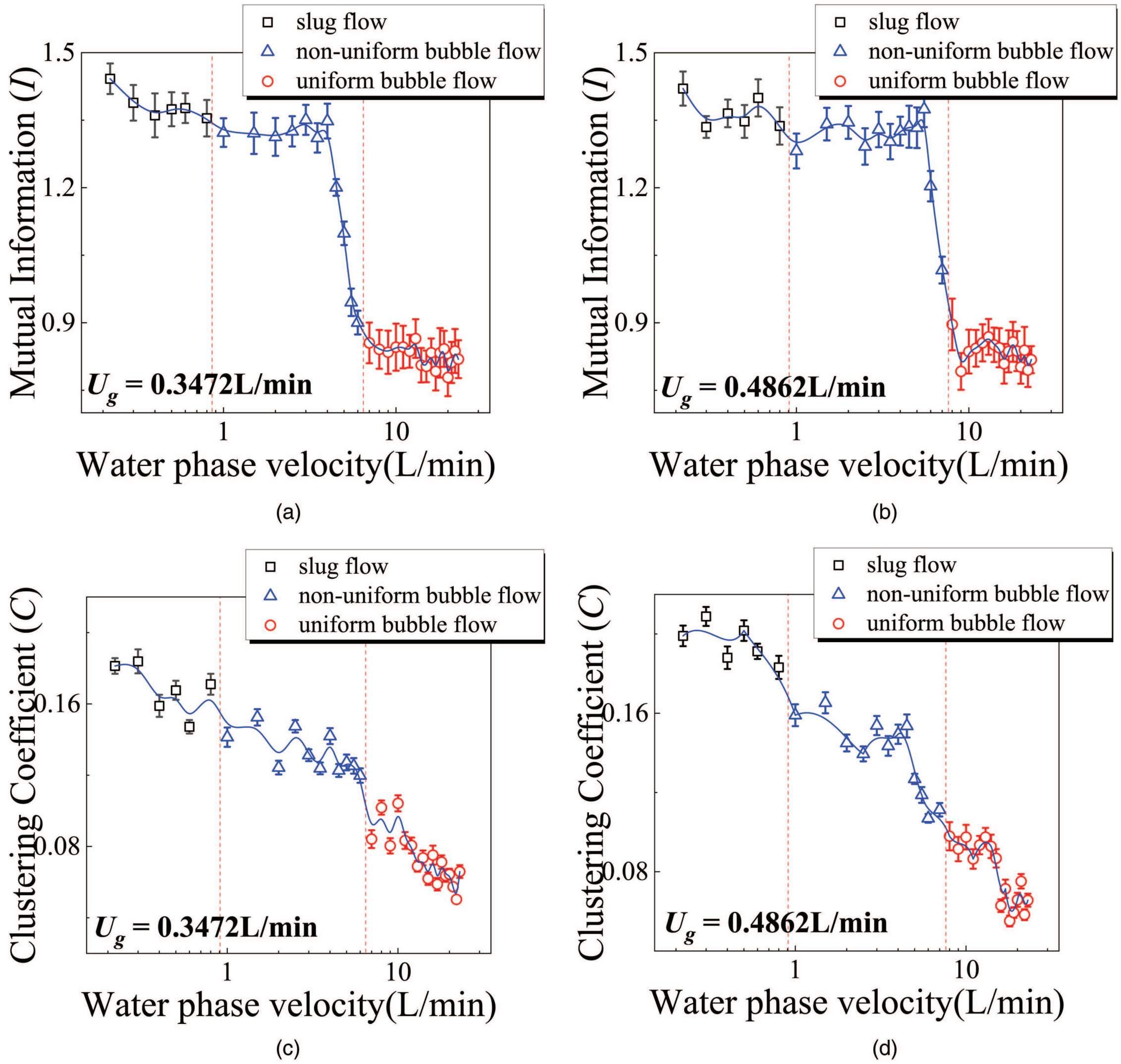

FIG. 6. The evolution of the global subnetwork mutual information I and the global subnetwork clustering coefficient C under different flow conditions.

the fluid turbulence intensity is so weak that the gas phase coalesces into gas slugs, which maintain a stable flow structure, resulting in a strong coupling flow behavior. With increasing the water flow velocity, the fluid turbulence is enhanced, and the gas slugs are broken into non-uniform bubbles, which exhibit diverse flow behaviors but still retain a rather stable flow structure. In this regard, the flow pattern spatial coupling strength of uniform bubble flow is gradually getting weaker with increasing the water velocity. At even higher water flow velocity, the fluid turbulence is strong enough to break the non-uniform bubbles into smaller uniformly distributed gas bubbles, which exhibit homogeneous flow behaviors. The flow behavior of uniform bubble flow shows stochastic characteristics, and the uniformly distributed small gas bubbles are weakly coupled with each other. We also find that the global mutual information I is sensitive to the phase transition.

As shown in Figs. 6(a) and 6(b), there exists a dramatic decrease in the value of I, which indicates that the flow pattern evolves from intermittent flow patterns (slug flow and non-uniform bubble flow) to the homogeneous flow pattern (uniform bubble flow). However, the mutual information I does not capture the dynamic changes from slug flow to non-uniform bubble flow. This is due to the fact that both the gas slugs and the non-uniform bubbles exhibit intermittent flow behavior, resulting in similar periodic fluid fluctuations. In fact, in some reports,[55,56] the non-uniform bubble flow pattern is defined as the bubble-slug transition flow. When the gas slugs are broken into non-uniform bubbles, the

08 December 2023 12:53:02

Published under an exclusive license by AIP Publishing

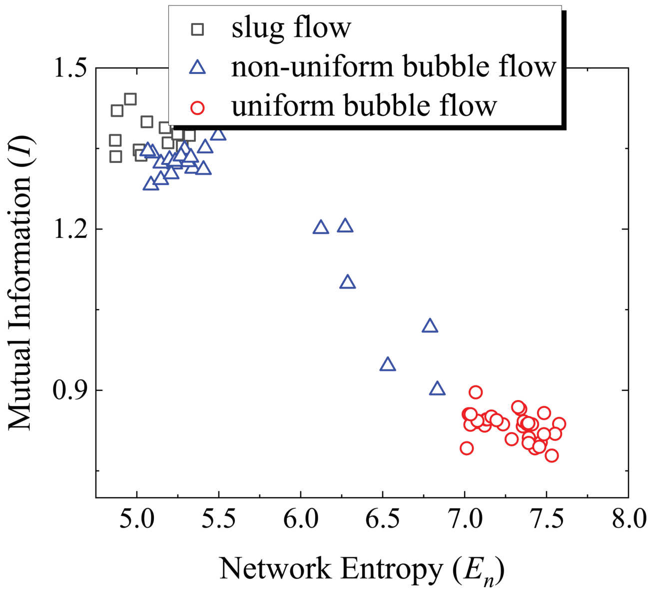

(a)

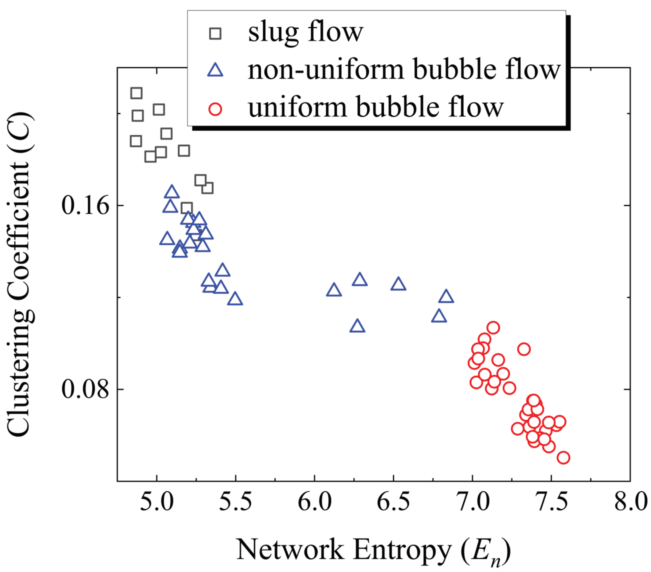

(b)

FIG. 7. The joint distributions of the network coupling indices and the complexity measure of the gas–liquid two-phase flow. (a) The joint distribution of the global subnetwork mutual information I and the global network entropy E. (b) The joint distribution of the global subnetwork clustering coefficient C and the global network entropy E.

global intermittent flow behavior is maintained by the periodically generated non-uniform bubbles. In particular, the clustering coefficient C quantifies the inter-subnetwork correlations of each node of the interconnected ordinal pattern complex network, and it characterizes the local coupling dynamics of a system. In this respect, as shown in Fig. 6, when increasing the water velocity, this measure is sensitive not only to flow pattern transitions but also to the subtle changes in flow behaviors within identical flow patterns.

To get a more detailed understanding of the gas–liquid two-phase flow spatial coupling behaviors, we carry out a joint analysis of the proposed coupling indices and the network complexity measure. We employ the global network entropy[43] as the complexity measure of the gas–liquid two-phase flow system. The network entropy of node i in subnetwork v^α is defined as

$$E_i^\alpha = -\sum_{j=1}^{p} d_{ij}^\alpha \cdot \log(d_{ij}^\alpha), \tag{17}$$

where d_{ij}^α denotes the weighted edge, which links the ith node to the jth node in the subnetwork v^α. The global network entropy E_n is then defined as

$$E_n = \frac{\sum_{\alpha=1}^{k}\sum_{i=1}^{p} E_i^\alpha}{k}, \tag{18}$$

where k is the number of subnetworks existing in the established interconnected ordinal pattern network.

The joint distributions of the network coupling indices and the complexity measure of the gas–liquid two-phase flow are shown in Fig. 7. We find that the flow pattern coupling strength and the fluid complexity are negatively correlated. When the flow pattern evolves from the slug flow to the uniform bubble flow, the coupling measures (I and C) gradually decrease, whereas the complexity measure of the fluid is gradually increasing. The slug flow, which is a typical periodical and intermittent flow pattern, exhibits obvious predictable flow behaviors, resulting in a lower complexity of the fluid. However, the stable structures of the gas slugs make the fluid maintaining strong spatial coupling behaviors, resulting in a higher value of the fluid coupling indices. When the flow pattern evolves to the uniform bubble flow, the flow behavior of small gas bubbles becomes stochastic and unpredictable. In this regard, the complexity measure of uniform bubble flow rises to a relatively higher value. Meanwhile, the flow behaviors of these uniform bubbles are independent and uncorrelated, which leads to the reduction of the coupling indices.

V. CONCLUSIONS

In this work, we investigate the spatial coupling behaviors of gas–liquid two-phase flow patterns by using experimental multivariate fluid conductance fluctuation signals. We first carry out a gas–liquid two-phase flow experiment in a vertical 50 mm inner diameter pipe to generate different flow patterns. Meanwhile, we employ a four-sector conductance sensor to collect the multivariate conductance fluctuation signals under different flow conditions. These signals are then used to reconstruct the interconnected ordinal pattern complex network, which is powerful for analyzing the evolutionary dynamics of the two-phase flow system. We also propose two coupling indices, which are the subnetwork mutual information (I) and the subnetwork clustering coefficient (C), to quantitatively analyze the spatial coupling behaviors of various gas–liquid two-phase flow patterns.

08 December 2023 12:53:02

Published under an exclusive license by AIP Publishing

We find that the coupling behaviors of the gas–liquid two-phase flow system are not only related to the flow patterns but also the fluid turbulence intensity. When the flow pattern evolves from the slug flow via the non-uniform bubble flow, to the uniform bubble flow, the fluid turbulence is enhanced, resulting in the spatial coupling strength of the gas–liquid two-phase flow gradually decreasing. In addition, we carry out a joint analysis of the proposed coupling indices and the network complexity measure. We find that the coupling strength of the gas–liquid two-phase flow system is negatively related to fluid complexity. The more complex the mixture fluid is, the weaker coupled the flow patterns are. Our research provides a new approach for characterizing the coupling behaviors of the two-phase flow system, and it is expected to find broader applications in complex systems with multiple observations.

ACKNOWLEDGMENTS

This work was supported in part by the Tianjin Technical Innovation Guidance Special Fund (No. 22YDTPJC00300), the Natural Science Foundation of Tianjin (No. 21JCJQJC00130), the National Natural Science Foundation of China (NNSFC) (Grant Nos. 61922062, 61873181, and 41704131), and the Taishan Industrial Experts Program.

AUTHOR DECLARATIONS

Conflict of Interest

The authors have no conflicts to disclose.

Ethics Approval

Ethics approval is not required.

Author Contributions

Meng Du: Project administration (lead); Writing – original draft (lead). **Jie Wei:** Investigation (lead); Software (lead); Visualization (lead). **Meng-Yu Li:** Methodology (lead). **Zhong-ke Gao:** Supervision (lead); Writing – review & editing (equal). **Jürgen Kurths:** Writing – review & editing (lead).

DATA AVAILABILITY

The data that support the findings of this study are available from the corresponding author upon reasonable request.

REFERENCES

[1] Y. H. Wu, L. S. Cheng, S. J. Huang, Y. H. Bai, P. Jia, S. R. Wang, B. X. Xu, and L. Chen, "An approximate semianalytical method for two-phase flow analysis of liquid-rich shale gas and tight light-oil wells," J. Pet. Sci. Eng. **176**, 562–572 (2019).
[2] P. I. Cano, J. Brito, F. Almenglo, M. Ramírez, J. M. Gómez, and D. Cantero, "Influence of trickling liquid velocity, low molar ratio of nitrogen-sulfur and gas-liquid flow pattern in anoxic biotrickling filters for biogas desulfurization," Biochem. Eng. J. **148**, 205–213 (2019).
[3] Y. J. Chang, Q. Xu, Q. H. Wu, X. Y. Zhao, B. Huang, Y. C. Wang, and L. J. Guo, "Experimental study of the hydraulic jump phenomenon induced by the downstream riser structure in a pipeline–riser system," Chem. Eng. Sci. **256**, 117687 (2022).
[4] L. Zha, M. J. Shang, M. Qiu, H. Zhang, and Y. H. Su, "Process intensification of mixing and chemical modification for polymer solutions in microreactors based on gas-liquid two-phase flow," Chem. Eng. Sci. **195**, 62–73 (2019).
[5] L. S. Zhai, J. Yang, and Y. Q. Wang, "An investigation of transition processes from transient gas–liquid plug to slug flow in horizontal pipe: Experiment and cost-based recurrence analysis," Nucl. Eng. Des. **379**, 111253 (2021).
[6] B. Wu, M. Firouzi, T. Mitchell, T. E. Rufford, C. Leonardi, and B. Towler, "A critical review of flow maps for gas-liquid flows in vertical pipes and annuli," Chem. Eng. J. **326**, 350–377 (2017).
[7] F. Dong, L. H. Li, and S. M. Zhang, "Flow status identification based on multiple slow feature analysis of gas-liquid two-phase flow in horizontal pipes," Meas. Sci. Technol. **32**, 055301 (2021).
[8] A. V. Chinak, A. E. Gorelikova, O. N. Kashinsky, M. A. Pakhomov, V. V. Randin, and V. I. Terekhov, "Hydrodynamics and heat transfer in an inclined bubbly flow," Int. J. Heat Mass Transfer **118**, 785–801 (2018).
[9] S. Baragh, H. Shokouhmand, and S. S. M. Ajarostaghi, "Experiments on mist flow and heat transfer in a tube fitted with porous media," Int. J. Therm. Sci. **137**, 388–398 (2019).
[10] C. S. Daw, C. E. A. Finney, M. Vasudevan, N. A. Van Goor, K. Nguyen, D. D. Bruns, E. J. Kostelich, C. Grebogi, E. Ott, and J. A. Yorke, "Self-organization and chaos in a fluidized bed," Phys. Rev. Lett. **75**, 2308 (1995).
[11] Z. Wu, Z. Cao, and B. Sunden, "Flow patterns and slug scaling of liquid-liquid flow in square microchannels," Int. J. Multiphase Flow **112**, 27–39 (2019).
[12] N. Zhao, C. F. Li, H. J. Jia, F. Wang, Z. Y. Zhao, L. D. Fang, and X. T. Li, "Acoustic emission-based flow noise detection and mechanism analysis for gas-liquid two-phase flow," Measurement **179**, 109480 (2021).
[13] H. Ziaei-Halimejani, S. Kouzbour, R. Zarghami, R. Sotudeh-Gharebagh, B. Gourich, N. Mostoufi, and Y. Stiriba, "Monitoring of the bubble columns hydrodynamics by recurrence quantification data analysis," Chem. Eng. Res. Des. **171**, 100–110 (2021).
[14] Z. K. Gao, D. M. Lv, W. D. Dang, M. X. Liu, and X. L. Hong, "Multilayer network from multiple entropies for characterizing gas-liquid nonlinear flow behavior," Int. J. Bifurcation Chaos **30**, 2050014 (2020).
[15] Q. M. Sun and B. Zhang, "Nonlinear characterization of gas liquid two-phase flow in complex networks," Exp. Therm. Fluid Sci. **60**, 165–172 (2015).
[16] W. Z. Liu, Q. Xu, S. F. Zou, Y. J. Chang, and L. J. Guo, "Optimization of differential pressure signal acquisition for recognition of gas–liquid two-phase flow patterns in pipeline-riser system," Chem. Eng. Sci. **229**, 116043 (2021).
[17] S. Wijayanta, Deendarlianto, Indarto, A. Prasetyo, and A. Z. Hudaya, "The effect of the liquid physical properties on the wave frequency and wave velocity of co-current gas-liquid stratified two-phase flow in a horizontal pipe," Int. J. Multiphase Flow **158**, 104300 (2023).
[18] W. K. Ren, J. C. Zhang, and N. D. Jin, "Rescaled range permutation entropy: A method for quantifying the dynamical complexity of gas-liquid two-phase slug flow," Nonlinear Dyn. **104**, 4035–4043 (2021).
[19] D. Li, M. Chen, S. Zhao, and A. W. Zeng, "Entropy generation analysis of Rayleigh convection in gas–liquid mass transfer process," Chem. Eng. Res. Des. **134**, 359–369 (2018).
[20] A. V. Cherdantsev, S. A. Zdornikov, M. V. Cherdantsev, S. V. Isaenkov, and D. M. Markovich, "Stratified-to-annular gas-liquid flow patterns transition in a horizontal pipe," Exp. Therm. Fluid Sci. **132**, 110552 (2022).
[21] L. S. Zhai, H. L. Xie, J. Yang, Y. L. Wu, and X. Z. Lu, "Characterizing dynamics of swirling film in gas-liquid cylindrical cyclone separator using multi-scale entropy analysis," Int. J. Mod. Phys. C **30**, 2050001 (2019).
[22] B. A. Khudayarov and K. M. Komilova, "Vibration and dynamic stability of composite pipelines conveying a two-phase fluid flows," Eng. Fail. Anal. **104**, 500–512 (2019).
[23] M. Du, L. Zhang, X. Y. Niu, and C. Grebogi, "Detecting gas-liquid two-phase flow pattern determinism from experimental signals with missing ordinal patterns," Chaos **30**, 093102 (2020).
[24] D. Diego, K. A. Haaga, and B. Hannisdal, "Transfer entropy computation using the Perron-Frobenius operator," Phys. Rev. E **99**, 042212 (2019).
[25] P. Sundaram, M. Luessi, M. Bianciardi, S. Stufflebeam, M. Hämäläinen, and V. Solo, "Individual resting-state brain networks enabled by massive multivariate conditional mutual information," IEEE Trans. Med. Imaging **39**, 1957–1966 (2019).

08 December 2023 12:53:02

Published under an exclusive license by AIP Publishing

[26] M. Rosenblum, M. Frühwirth, M. Moser, and A. Pikovsky, "Dynamical disentanglement in an analysis of oscillatory systems: An application to respiratory sinus arrhythmia," Philos. Trans. R. Soc. A **377**, 20190045 (2019).

[27] J. L. Neri, P. Depalle, and R. Badeau, "Approximate inference and learning of state space models with Laplace noise," IEEE Trans. Signal Process. **69**, 3176–3189 (2021).

[28] D. Wang, D. T. Ren, K. Li, Y. M. Feng, D. Ma, X. G. Yan, and G. Wang, "Epileptic seizure detection in long-term EEG recordings by using wavelet-based directed transfer function," IEEE Trans. Biomed. Eng. **65**, 2591–2599 (2018).

[29] F. Goetze and P. Y. Lai, "Reconstructing positive and negative couplings in Ising spin networks by sorted local transfer entropy," Phys. Rev. E **100**, 012121 (2019).

[30] R. Malladi, D. H. Johnson, G. P. Kalamangalam, N. Tandon, and B. Aazhang, "Mutual information in frequency and its application to measure cross-frequency coupling in epilepsy," IEEE Trans. Signal Process. **66**, 3008–3023 (2018).

[31] D. Wen, P. L. Jia, S. H. Hsu, Y. H. Zhou, X. F. Lan, D. Cui, G. L. Li, S. M. Yin, and L. Wang, "Estimating coupling strength between multivariate neural series with multivariate permutation conditional mutual information," Neural Netw. **110**, 159–169 (2019).

[32] J. F. Fan, J. Meng, J. Ludescher, X. S. Chen, Y. Ashkenazy, J. Kurths, S. Havlin, and H. J. Schellnhuber, "Statistical physics approaches to the complex earth system," Phys. Rep. **896**, 1–84 (2021).

[33] Y. Zou, R. V. Donner, N. Marwan, J. F. Donges, and J. Kurths, "Complex network approaches to nonlinear time series analysis," Phys. Rep. **787**, 1–97 (2019).

[34] T. Kobayashi, S. Murayama, T. Hachijo, and H. Gotoda, "Early detection of thermoacoustic combustion instability using a methodology combining complex networks and machine learning," Phys. Rev. Appl. **11**, 064034 (2019).

[35] C. Tan, W. L. Liu, and F. Dong, "Characterizing the correlations between local phase fractions of gas–liquid two-phase flow with wire-mesh sensor," Philos. Trans. R. Soc. A **374**, 20150335 (2016).

[36] C. Ma, Q. R. Yang, X. Q. Wu, and J. A. Lu, "Cluster synchronization: From single-layer to multi-layer networks," Chaos **29**, 123120 (2019).

[37] K. W. Li, M. X. Yu, L. Liu, J. N. Zhai, and W. Y. Liu, "A novel reliability analysis approach for component-based software based on the complex network theory," Soft. Test. Verif. Rel. **28**, e1674 (2018).

[38] O. Cats, G. J. Koppenol, and M. Warnier, "Robustness assessment of link capacity reduction for complex networks: Application for public transport systems," Reliab. Eng. Syst. Safe. **167**, 544–553 (2017).

[39] S. Scarsoglio, F. Cazzato, and L. Ridolfi, "From time-series to complex networks: Application to the cerebrovascular flow patterns in atrial fibrillation," Chaos **27**, 093107 (2017).

[40] B. Zarei, M. R. Meybodi, and B. Masoumi, "Chaotic memetic algorithm and its application for detecting community structure in complex networks," Chaos **30**, 013125 (2020).

[41] J. F. Donges, H. C. H. Schultz, N. Marwan, Y. Zou, and J. Kurths, "Investigating the topology of interacting networks," Eur. Phys. J. B **84**, 635–651 (2011).

[42] Z. K. Gao, M. X. Liu, W. D. Dang, C. Ma, L. H. Hou, and X. L. Hong, "Multilayer limited penetrable visibility graph for characterizing the gas-liquid flow behavior," Chem. Eng. J. **407**, 127229 (2021).

[43] M. Small, "Complex networks from time series: Capturing dynamics," in *2013 IEEE International Symposium on Circuits and Systems (ISCAS)* (IEEE, 2013), pp. 2509–2512.

[44] M. Huang, Z. K. Sun, R. V. Donner, J. Zhang, S. G. Guan, and Y. Zou, "Characterizing dynamical transitions by statistical complexity measures based on ordinal pattern transition networks," Chaos **31**, 033127 (2021).

[45] C. W. Kulp, J. M. Chobot, H. R. Freitas, and G. D. Sprechini, "Using ordinal partition transition networks to analyze ECG data," Chaos **26**, 073114 (2016).

[46] Y. J. Ruan, R. V. Donner, S. G. Guan, and Y. Zou, "Ordinal partition transition network based complexity measures for inferring coupling direction and delay from time series," Chaos **29**, 043111 (2019).

[47] W. Kobayashi, H. Gotoda, S. Kandani, Y. Ohmichi, and S. Matsuyama, "Spatiotemporal dynamics of turbulent coaxial jet analyzed by symbolic information-theory quantifiers and complex-network approach," Chaos **29**, 123110 (2019).

[48] Y. Nomi, H. Gotoda, S. Fukuda, and C. Almarcha, "Complex network analysis of spatiotemporal dynamics of premixed flame in a Hele–Shaw cell: A transition from chaos to stochastic state," Chaos **31**, 123133 (2021).

[49] Y. Nomi, H. Gotoda, S. Kandani, and C. Almarcha, "Complex network analysis of the gravity effect on premixed flames propagating in a Hele-Shaw cell," Phys. Rev. E **103**, 022218 (2021).

[50] Z. K. Gao, Y. X. Yang, L. S. Zhai, N. D. Jin, and G. R. Chen, "A four-sector conductance method for measuring and characterizing low-velocity oil–water two-phase flows," IEEE Trans. Instrum. Meas. **65**, 1690–1697 (2016).

[51] F. Takens, "Detecting strange attractors in turbulence," in *Dynamical systems and turbulence, Warwick 1980* (Springer, 1981), pp. 366–381.

[52] C. Bandt and B. Pompe, "Permutation entropy: A natural complexity measure for time series," Phys. Rev. Lett. **88**, 174102 (2002).

[53] M. B. Kennel, R. Brown, and H. D. I. Abarbanel, "Determining embedding dimension for phase-space reconstruction using a geometrical construction," Phys. Rev. A **45**, 3403 (1992).

[54] H. S. Kim, R. Eykholt, and J. D. Salas, "Nonlinear dynamics, delay times, and embedding windows," Physica D **127**, 48–60 (1999).

[55] G. F. Hewitt, *Measurement of Two Phase Flow Parameters* (Academic, New York, 1978).

[56] Z. K. Gao and N. D. Jin, "Flow-pattern identification and nonlinear dynamics of gas-liquid two-phase flow in complex networks," Phys. Rev. E **79**, 066303 (2009).

08 December 2023 12:53:02

Published under an exclusive license by AIP Publishing